Computers in Biology and Medicine 169 (2024) 107799

Contents lists available at ScienceDirect

Computers in Biology and Medicine

journal homepage: www.elsevier.com/locate/compbiomed

Evaluating computed bony range of motion (BROM) by registering in-vitro cadaver-based functional range of motion (FROM) to a hip motion simulation

Arnab Palit [a,*], Mark A. Williams [a], Ercihan Kiraci [a], Vineet Seemala [a], Vatsal Gupta [d], Jim Pierrepont [b], Christopher Plaskos [c], Richard King [d]

[a] WMG, The University of Warwick, Coventry, UK
[b] Corin Ltd, Corinium Centre, Cirencester, Gloucestershire, GL7 1YJ, UK
[c] Corin Ltd., Raynham, MA, USA
[d] Department of Trauma & Orthopaedics, University Hospitals Coventry and Warwickshire NHS Trust, Coventry, UK

ARTICLE INFO

Keywords:
Hip range of motion
Bony impingement
Motion measurement
Functional range of motion
Activities of daily living (ADLs)
Soft tissue
Ligaments

ABSTRACT

Background: While modern hip replacement planning relies on hip motion simulation (HMS), it lacks the capability to include soft-tissues and ligaments restraints on computed bony range of motion (BROM), often leading to an overestimation of the in-vivo functional range of motion (FROM). Furthermore, there is a lack of literature on BROM assessment in relation to FROM. Therefore, the study aimed to assess computed BROM using in-vitro cadaver-derived FROM measurements, registered to a CT-based in-house HMS, and to further investigate the effect of functional and anatomical hip joint centres (FHJC and AHJC) on BROM.

Method: Seven limiting and three non-limiting circumducted passive FROM of four cadaver hips were measured using optical coordinate measuring machine with reference spheres (RSs) affixed to the pelvis and the femur, following CT-scan of the specimen. The RSs' centres were used to register the measured FROM in HMS, enabling its virtual recreation to compute corresponding BROM by detecting nearest bony impingement. FHJC, estimated from non-limiting FROM, was compared with AHJC to examine their positional differences and effect on BROM.

Results: Differences in BROM and FROM were minimal in deep flexion (3.0° ± 4.1°) and maximum internal rotation (IR) at deep flexion (3.0° ± 2.9°), but substantially greater in extension (53.2° ± 9.5°). Bony impingement was observed during flexion, and IR at deep flexion for two hips. The average positional difference between FHJC and AHJC was 3.1 ± 1.2 mm, resulting in BROM differences of 1°–13° across four motions.

Conclusions: The study provided greater insight into the applicability and reliability of computed BROM in pre-surgical planning.

1. Introduction

Total Hip Arthroplasty (THA) is one of the most commonly performed procedures in orthopaedic surgery [1]. It aims to restore function and mobility of the hip joint which has been affected by osteoarthritis (OA), rheumatoid arthritis (RA), and acute trauma [2,3]. Impingement following THA is associated with inadequate range of motion (ROM), greater risk of dislocation, component wear and various other complications that ultimately lead to patient dissatisfaction [4,5] and the need for revision surgery. There are many factors that influence the risks of impingement and dislocation, including implant design, implant position, type of surgical approach, bony structures around the hip and other patient related characteristics such as gender, age, and history of previous hip surgery [6–10]. Various mitigation strategies are therefore employed to reduce post-THA complications, such as careful pre-operative planning, thorough intra-operative assessments, and meticulous post-operative care [11]. In terms of pre-operative THA planning, hip motion simulation (HMS) is now being used to assess ROM and predict post-THA implant-to-implant impingement (ITI) [12–17] and bony impingement (BI) [18–20] to identify best possible implant positions.

HMS generally uses CT images (or MRI images) to construct the

* Corresponding author. WMG, University of Warwick, Coventry, CV4 7AL, UK.
E-mail addresses: a.palit.1@warwick.ac.uk, arnabpalit@gmail.com (A. Palit).

https://doi.org/10.1016/j.compbiomed.2023.107799
Received 18 September 2023; Received in revised form 9 November 2023; Accepted 29 November 2023
Available online 4 December 2023

geometry of the pelvis and femur, and thereafter simulate hip ROM to estimate implant and bony impingement [12–16,18,19,21]. However, one of the major limitations of pre-planning simulation is that it cannot incorporate the effects of the soft tissues and ligaments on simulated bony range of motion (BROM). Therefore, the BROM values reported through the simulation tends to overestimate the actual in-vivo functional range of motion (FROM) [21,22] of a hip that is further constrained by soft tissues and ligaments. Although CT-based HMS is a cost-effective and time-efficient method to be used in conjunction with the clinical settings, the validity of the calculated limiting BROM is not well described in the literature, specifically in the context of comparing it with measured FROM. Consequently, this hinders the ability to identify BROMs which are close representation of actual FROM and could be used as subject-specific target values for surgical pre-planning. Therefore, development of a method to evaluate computed BROM of a healthy and normal hip anatomy in relation to its actual FROM is a crucial step in achieving the broader goal of uncovering the relationship between BROMs and FROMs.

Previous works validated the hip ROM simulation using secondary clinical case studies with controlled patient groups [19,20] or synthetic models [23–25] which did not depict the actual FROM measurement. Few studies measured the effect of soft-tissue impingement intra-operatively during posterior approach THA [26], and anterolateral approach THA [27] using CT-based or imageless navigation system respectively. However, these were post-surgery measurement, and it did not directly compare the FROM with the simulated BROM of healthy and normal hip anatomy. A few studies measured selected manoeuvres in cadavers and combined them with simulated BROM [22,24,28] for validation. However, anatomical landmarks that were used for registration in these studies were identified either by dissecting the soft tissue [24] or inserting Kirchner-wires with electromagnetic tracking system (EMTS) [28]. As these landmarks were individual points, any error in detecting these points (during measurement or from CT-scan) would introduce substantial errors in the registration process. This would ultimately lead to greater error in the comparison results between FROM and simulated hip BROM. Additionally, none of these studies investigated the sensitivity of the comparative results due to the variation in the registration process. On the other hand, hip joint centre (HJC) is an important landmark to simulate and estimate limiting BROM. It represents the centre of rotation around which hip motion occurs. In general, anatomical hip joint centre (AHJC) is used in HMS [21]. AHJC is a centre of a best fit sphere on CT derived femoral head geometry. However, actual hip motion occurs with respect to the functional hip joint centre (FHJC) which is generally determined through mathematical algorithms that consider the dynamic motions of two adjacent segments (in this case, pelvis and femur). Therefore, use of FHJC in simulation requires actual hip motion measurement, and subsequent estimation of FHJC. This is not possible during pre-planning stage and in pre-operative clinical environment. AHJC is used, therefore, in HMS, even though AHJC and FHJC may not always be located exactly at the same position. As a result, the estimated limiting BROM would be different, depending on whether AHJC or FHJC was used in the simulation. To the best of the authors' knowledge, this effect of using AHJC instead of FHJC in simulation and hip ROM calculation has never been investigated in the literature.

Therefore, the purpose of this study was to develop an accurate and precise method to measure FROM using cadaver specimen, and subsequently register the measured FROM to a CT-based in-house HMS to validate the estimated BROM of a normal and healthy hip anatomy. Specific objectives associated with this work were as follows: (a) Development of the experimental procedure to measure FROM using cadaver specimen with capability to accurately and precisely register the measured FROM to a CT-based in-house HMS tool; (b) Validation of the simulation method by comparing the measured FROMs and corresponding computed BROMs; (c) Assessment of its sensitivity in relation to variations in the registration process; and finally, (d) Identification of the positional difference between FHJC and AHJC, and their impact on the computed BROM values in HMS. The following section outlines the materials and methods employed in this study, including the specimen preparation, experimental setup, FROM measurement procedure, the development of in-house HMS, the method to register FROM into HMS along with factors influencing the registration process, the computation of corresponding BROM to the measured FROM, and the methodology for examining the impact on computed BROM due to the use of FHJC and AHJC. Subsequently, the results section discusses the measured FROM values, compares them with the calculated BROM, underscores the sensitivity arising from registration errors, and ultimately presents the influence of FHJC and AHJC on the computed BROM. This is followed by the discussion and conclusion section.

2. Material and methods

This study involved experimental measurement of four cadaveric hips, followed by registering the measured hip movement to a HMS, generated from post-experiment CT scans.

2.1. Specimens preparation and experimental set-up

Two cadaveric specimens, transected from the L5 vertebra to the feet, consisting of four cadaveric hips, were obtained from two donors. X-rays was performed to screen for any evidence of arthritis and other pathologic conditions such that the measurements were performed only on normal/healthy hips. Both the cadavers were male, with ages 71 and 78 years. The study was approved by Research and Development, University Hospitals Coventry and Warwickshire (UHCW) NHS Trust (Ref: GF0503), and Biomedical & Scientific Research Ethics Committee (BSREC) at University of Warwick (ref: BSREC 66/22–23). The experimental set-up is shown in Fig. 1.

To facilitate the placement of the cadaver specimen, a specially designed fixation plate (Fig. 1a and b) was manufactured at the WMG workshop, University of Warwick. The plate was designed with provisions for attaching two C-clamps, which were used to secure the cadaver specimen in place. The dimensions of the plate were carefully designed to ensure that it did not restrict the extension movement of the hip. Furthermore, the fixation plate was affixed to a surgical table that offered adjustable height settings. The feet of the specimen were positioned on separate tables either during the resting position or when performing measurements on the contralateral side.

In this study, AICON MoveInspect XR8 (AICON, Hexagon, UK), a camera-based portable coordinate measuring machine (CMM) with a capability of 'Dynamic Referencing', was used to measure FROM (Fig. 1d). The CMM consists of a camera beam and two 8 megapixels calibrated XR cameras. The equipment also included an optically tracked handheld probing device, while the MoveInspect software determined the 3D coordinates of object points or the six degrees of freedom (6 DoF) data of solid bodies at an acquisition frequency of 5 Hz. The specified measurement range of 1–3 m (6.7 m^3) was used during the experiment. The accuracy and the precision of the measurement system were 20 μm + 30 μm/m and 5 μm + 20 μm/m, respectively. Since the system only detects 2D markers, a specially designed 3D printed dome-shaped 'Femoral Adaptor' (similar to a truncated icosahedron shape) was manufactured at the WMG workshop, University of Warwick (Fig. 1c). The flat surface areas of the 'Femoral Adaptor' were covered with 2D markers. A coordinate system associated with the 'Femoral Adaptor' was determined by measuring the positions of all the 2D markers on it using AICON DPA (Digital Photogrammetry) series camera. The 'Femoral Adaptor' covered with markers was then rigidly affixed to the distal shaft of the femur using two 4 mm threaded surgical pins, external fixation clamps (Hoffman 3, Stryker®), and plastic glue. Similarly, the 'Pelvis Adaptor' was made of a plastic plate and covered with 2D markers. It was attached to the pelvis rigidly at the iliac crests using six 4 mm or 5 mm surgical pins, external fixation clamps and bars

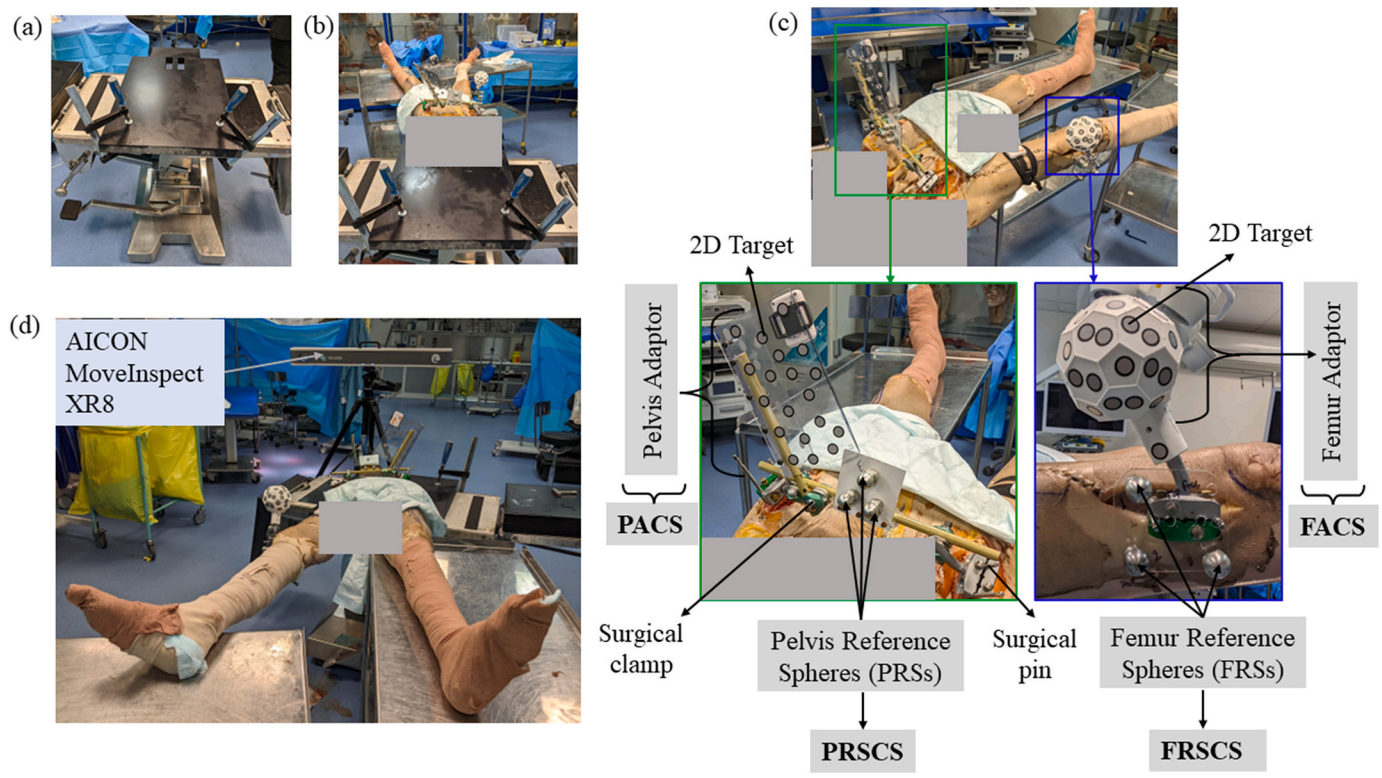

Fig. 1. Experimental set-up for the cadaver experiment. (a) A specially designed fixation plate is used to position the cadaver specimen. (b) The cadaver specimen is secured to the fixation plate using a C-clamp, and the fixation plate is clamped onto a height-adjustable table. (c) 'Pelvis Adaptor' and pelvis reference spheres (PRSs) are attached to the pelvis. They serve to establish the pelvis adaptor coordinate system (PACS) and pelvis reference sphere coordinate system (PRSCS), respectively. Similarly, 'Femur Adaptor' and femur reference spheres (FRSs) are affixed to the femur, providing the femur adaptor coordinate system (FACS) and femur reference sphere coordinate system (FRSCS), respectively. Surgical clamps, pins, and plastic glue are employed to secure these attachments to the pelvis and femur. (d) The final experiment setup is depicted, along with the positioning of the AICON MoveInspect XR8 during the experiment.

(Hoffman 3, Stryker®), and plastic glue, as shown in Fig. 1c. During femoral movement, the AICON MoveInspect XR8 system tracked the markers on the 'Femoral Adaptor' to accurately capture the position and orientation of the coordinate system linked to the 'Femoral Adaptor' in relation to the coordinate system associated with the 'Pelvis Adaptor'. Therefore, the system actually measured the relative position of the femur with respect to the pelvis.

Although CT scanning of the femoral adaptor and plastic plates was possible, they lacked distinguishable features that could be easily segmented for the purpose of registering the measured manoeuvre to the HMS. Therefore, a solution was implemented by rigidly attaching three metrological graded Alufix 'reference balls' (Alufix, reference ball id 28403-1, 18 mm diameter, Aluminium) to the femoral bone (distal part of the femur) using surgical pins, clamps, and screws, as depicted in Fig. 1c. Similarly, three Alufix 'reference balls' were also affixed to pelvis by attaching them on a connecting rod that was fixed to the clamps, affixed rigidly to the iliac crest area of the pelvis as illustrated in Fig. 1c. These spherical 'reference balls' served as reliable points of reference, as their centres could be accurately and precisely measured by both the AICON System and post-experiment CT scans. This ensured the availability of consistent and accurate data to register the measured FROM into HMS. The spherical 'Reference balls' that were rigidly attached to the femur and pelvis are referred to as the 'femur reference spheres' (FRSs) and the 'pelvis reference spheres' (PRSs), respectively in this paper.

2.2. Experimental procedure to measure FROM

Prior to commencing the measurements, calibration of the AICON MoveInspect XR8 and the probing device were performed using a reference rod and probe tip reference sphere, respectively. Subsequently, the surface points of FRS were measured using the touch probe device to accurately determine the centres of the FRS. This was achieved by fitting a sphere to the measured surface points of the FRS through a best-fit method in SpatialAnalyzer software (SA, 2019.09.10 Version). The centre points of the femur reference spheres (FRSs) were subsequently utilised to establish the femur reference sphere coordinate system (FRSCS). Thereafter, the position and orientation of the femoral adaptor coordinate system (FACS) in relation to the femur reference sphere coordinate system (FRSCS) in the resting position was measured using the AICON camera for a duration of 5s. This provided the transformation matrix ${}^{FACS}T_{FRSCS}$ to define the relation between these two coordinate systems. Similarly, pelvis reference sphere coordinate system (PRSCS) was defined by using the centre points of pelvis reference spheres (PRSs). Subsequently, the relation between pelvis reference sphere coordinate system (PRSCS) and pelvis adaptor coordinate system (PACS), which was associated with the pelvis adaptor, was established through ${}^{PACS}T_{PRSCS}$. Thereafter, the position and orientation of the femoral adaptor coordinate system (FACS) were recorded relative to the pelvis adaptor coordinate system (PACS) during the passive movement of the femur. By utilising the relationship between pelvis adaptor and pelvis reference sphere coordinate system, (PACS and PRSCS i.e., ${}^{PACS}T_{PRSCS}$), the position and orientation of femoral adaptor coordinate system (FACS) were expressed in relation to pelvis reference sphere coordinate system (PRSCS) (${}^{PRSCS}T_{FACS}(t)$) for the measurement duration t.

Initially, a non-limiting circumducted motion (or conical motion) of the femur was executed. The term 'non-limiting' was used to highlight that there was no chance of impingement during these mid-range circumducted motions. This motion was performed freehand three times.

The collected data from these measurements were used to calculate the FHJC. The reliability of estimating the FHJC was assessed based on the three sets of measurement runs. Thereafter, the hip joint was moved passively to the end of its range as assessed by an experienced orthopaedic surgeon (RK) to define the 'limiting' passive FROM. In the experiment, seven limiting passive FROM were performed which were clinically relevant as follows: (1) maximum flexion (flex), (2) maximum extension (extn), (3) maximum abduction (abd), (4) maximum internal rotation (IR) in deep flexion with minimal abduction/adduction (abd/add), (5) maximum IR in deep flexion in maximal abduction, (6) maximum IR at deep flexion in maximal adduction, (7) maximum external rotation (ER) in full extension with various positions of abduction/adduction. In the case of deep flexion, the flexion range was in between 70° and 100°. On the other hand, minimal abduction/adduction represented a range of 0–15°, while maximal abduction/adduction corresponded to more than 15°. Each manoeuvre was held for 5 s in the limiting position, during which measurements were taken. All these limiting manoeuvres were repeated three times by an experienced orthopaedic surgeon (RK) to ensure consistency.

2.3. Hip ROM simulation

3D geometries of pelvis and femur were created from post-experiment CT images along with the identification of bony landmarks using Simpleware™ ScanIP software (Version 2022, Synopsys, Inc., Mountain View, USA). The workflow involved importing DICOM CT images into ScanIP, followed by cubic/isotropic resampling and defining the region of interest. The pelvis and femur were then semi-automatically segmented by applying lower and upper grayscale threshold values, after which a morphological closing operation was applied to close any holes and remove any islands within the segmented masks. Finally, a 3D geometry was constructed from the mask and subsequently exported as STL files for use in the simulation [21]. During the construction of the STL files, the maximum edge length of the surface triangles was kept below 1.5 mm to ensure consistent quality among the generated geometries utilised in bony impingement detection. Four landmarks were identified for pelvis as follows (Fig. 2a): (a) right anterior superior iliac spines ($ASIS_{Right}$), (b) left anterior superior iliac spines ($ASIS_{Left}$), (c) right pubic tubercles ($PTUB_{Right}$), (d) left pubic tubercles ($PTUB_{Left}$) [21,29]. In terms of femur geometry, three landmarks were identified: (Fig. 2b), (a) femoral head centre, (b) lateral epicondyle. ($EPI_{Lateral}$), (c) medial epicondyle. (EPI_{Medial}) [21]. The femoral head centre was determined as the centre of the best fit sphere on the femoral head [21]. In the simulation, the femoral head centre was considered as anatomical hip joint centre (AHJC) [21]. The Pelvic Coordinate System (PCS) and Femoral Coordinate System (FCS) were constructed using the four pelvic and three femoral landmarks respectively (Fig. 2c) according to the ISB recommendation [30] as described below.

Firstly, Anterior Pelvic Plane (APP) was defined using three landmark points – $ASIS_{Right}$, $ASIS_{Left}$, and $PTUB_{Mid}$ which is the midpoint of $PTUB_{Right}$ and $PTUB_{Left}$ (Fig. 2a). The medial-lateral x-axis (X_P) was determined by a line connecting $ASIS_{Left}$ and the $ASIS_{Right}$ where the positive direction followed $ASIS_{Right}$ to $ASIS_{Left}$. The y-axis (Y_P), representing the anterior-posterior direction, was orthogonal to the APP, with its positive direction indicating posterior to anterior. Finally, the z-axis (Z_P) denoted the superior-inferior direction and was orthogonal to both X_P and Y_P axes. The positive z-axis denoted inferior to superior direction to complete the definition of PCS.

The FCS was defined as follows (Fig. 2b). Knee centre (KC) was determined by the mid-point of $EPI_{Lateral}$ and EPI_{Madial}. The superior-inferior z-axis (Z_F) was a line running in the positive direction from the KC to the HJC. The anterior-posterior y-axis (Y_F), with its positive direction indicating posterior to anterior, was defined by a normal to a plane that was defined by three points – HJC, $EPI_{Lateral}$ and EPI_{Madial}. The medial-lateral x-axis (X_F) was orthogonal to the other two axes.

The rotation matrix of PCS and FCS with respect to the world coordinate system (WCS) is therefore represented by the rotation matrix R_P^W and R_F^W respectively in Eq. (1) where the superscript represent i, j, and k component of each unit vector X_F, Y_F, and Z_F. The origin of both PCS and FCS was defined by the AHJC at the neutral position.

$$R_P^W = \begin{bmatrix} X_P^i & Y_P^i & Z_P^i \\ X_P^j & Y_P^j & Z_P^j \\ X_P^k & Y_P^k & Z_P^k \end{bmatrix}; R_F^W = \begin{bmatrix} X_F^i & Y_F^i & Z_F^i \\ X_F^j & Y_F^j & Z_F^j \\ X_F^k & Y_F^k & Z_F^k \end{bmatrix} \quad (1)$$

The PCS and FCS were not necessarily aligned together when they were constructed using the input landmarks (Fig. 2c) that was identified

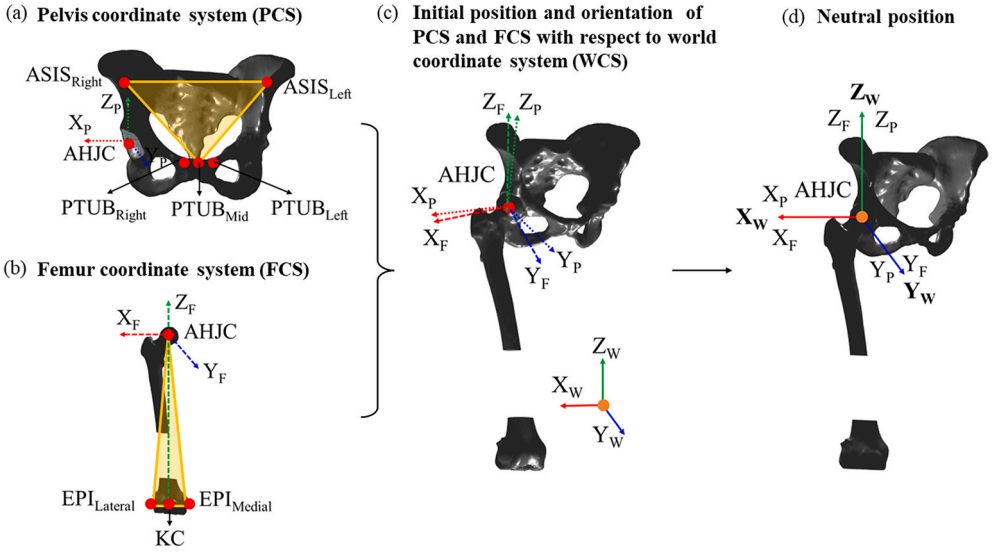

Fig. 2. Determination of Pelvic Coordinate System (PCS) and Femur Coordinate System (FCS) from the landmarks and alignment of PCS and FCS to the World Coordinate System (WCS); (a) schematic representation of four pelvic landmarks ($ASIS_{Right}$, $ASIS_{Left}$, $PTUB_{Right}$, $PTUB_{Left}$), definition of APP and PCS (X_P, Y_P, Z_P) with origin at AHJC; (b) schematic representation of two femoral landmarks ($EPI_{Lateral}$, and EPI_{Madial}), Knee Centre, and the definition of FCS (X_F, Y_F, Z_F) with origin at AHJC; (c) schematic representation of the PCS and FCS to show that these coordinate systems might not be aligned with each other and with WCS (X_W, Y_W, Z_W) initially; (d) alignment of PCS and FCS to WCS to define the neutral position of pelvis and femur.

from the CT-scan images of hip in supine position. To address this, the pelvis and femur geometries were initially translated, ensuring that the Anatomical Hip Joint Centre (AHJC) coincided with the origin of the World Coordinate System (WCS). Subsequently, the pelvis geometry was rotated using the transpose of the rotation matrix R_P^W i.e., $(R_P^W)^T$ to align PCS with WCS. These adjustments ensured that X_P and Y_P coincided with X_W and Y_W respectively (Fig. 2d). Similarly, FCS and WCS were aligned by rotating the femur geometry using transpose of the rotation matrix R_F^W i.e., $(R_F^W)^T$ so that X_F and Y_F coincided with X_W and Y_W respectively (Fig. 2d). This position was termed as neutral position where PCS, FCS and WCS were coincident (Fig. 2d).

To determine the limiting BROM, the study employed the method developed by Palit, King [20]. The radius of the best fit sphere, which was created to determine AHJC, was incrementally enlarged with very small step size (0.1 mm) until it encompassed the entire femoral head. This expansion allowed the sphere to intersect the femur precisely into two regions: (a) the femoral head and (b) the remaining geometry of the femur. By employing this condition and using such a small step size (0.1 mm), the variations in the dimensions of the expanded sphere were negligible. Subsequently, two distinct geometries were then used for the identification of bony impingement: the entire pelvis and the femur with the resected head. As the spherical articular surface of the femoral head does not impinge with the acetabulum during the motion of a healthy hip, this region was excluded from the analysis. The pure joint motion of the femur (with resected head) was then defined as follows: (a) R_x represented the rotation with respect to global x-axis (X_W) to generate flexion-extension movement of angle α, (b) R_y depicted the rotation around global y-axis (Y_W) to generate abduction-adduction of angle β, and (c) R_z created the rotation around global z-axis (Z_W) to generate internal-external rotation of angle γ.

$$R_x = \begin{bmatrix} 1 & 0 & 0 \\ 0 & cos\,\alpha & -sin\,\alpha \\ 0 & sin\,\alpha & cos\,\alpha \end{bmatrix};$$
$$R_y = \begin{bmatrix} cos\,\beta & 0 & sin\,\beta \\ 0 & 1 & 0 \\ -sin\,\beta & 0 & cos\,\beta \end{bmatrix};$$
$$R_z = \begin{bmatrix} cos\,\gamma & -sin\,\gamma & 0 \\ sin\,\gamma & cos\,\gamma & 0 \\ 0 & 0 & 1 \end{bmatrix} \quad (1)$$

Any combined hip joint motion of femur was represented as a multiplication of these matrices in a given sequence. In this study, the following intrinsic rotation sequence was used to represent the combined hip motion: $R_{comb} = Rx*Ry*Rz$. To calculate the limiting BROM, a collision check function was used in Matlab using the MEX API interface. This function was developed by leveraging the 'collision detection' algorithm provided by the Proximity Query Package (PQP) library [44]. To verify its accuracy, the output of this function, which consisted of intersection points, was compared to the intersection points computed by Mimics 3-matic software when the same STL geometries were utilised [20]. The comparison revealed a high degree of similarity between the output points, thus affirming the reliability of the function.

2.4. Registration of FROM to hip ROM simulation

The centre points of femur reference spheres (FRS) and pelvis reference spheres (PRS) were identified from the post-CT segmentation, following best-fit sphere method using Simpleware™ ScanIP software (Synopsys, Inc., Mountain View, USA). These centre points were used to define femur reference sphere coordinate system (FRSCS) and pelvis reference sphere coordinate system (PRSCS) in CT world coordinate (CTW) which were referred as ${}^{CTW}T_{FRSCS}$ and ${}^{CTW}T_{PRSCS}$ respectively. Furthermore, the relation between pelvis reference sphere coordinate system (PRSCS) and pelvis coordinate system (PCS) was defined by ${}^{PRSCS}T_{PCS}$. Similarly, ${}^{FRSCS}T_{FCS}$ represented the relation between femur reference sphere coordinate system (FRSCS) and femur coordinate system (FCS). Since the measured passive FROM of the femur with respect to pelvis reference sphere coordinate system (PRSCS) for tth time was represented by the rotation matrix ${}^{PRSCS}T_{FACS}\,(t)$ (Section 2.2), the measurement data was registered to CTW coordinate system as follows (Eq. (2))

$${}^{CTW}T_{FACS}\,(t) = {}^{CTW}T_{PRSCS} * {}^{PRSCS}T_{FACS}\,(t) \quad (2)$$

Using the relation between FACS and FRSCS, the position of the FRS at tth time was calculated as (Eq (3))

$${}^{CTW}T_{FRSCS}\,(t) = {}^{CTW}T_{FACS}\,(t) * {}^{FACS}T_{FRSCS} \quad (3)$$

Finally, the position of the femur with respect to pelvis in CTW coordinate system was calculated as

$${}^{CTW}T_{FCS}\,(t) = {}^{CTW}T_{FRSCS}\,(t) * {}^{FRSCS}T_{FCS} \quad (4)$$

The rotational part of the transformation matrix ${}^{CTW}T_{FCS}\,(t)$ was then decomposed into x-y-z Euler angles where first Euler angle represented hip flexion/extension, second Euler angle represented hip abduction/adduction, and third Euler angle referred to internal or external rotation. This provided the limiting passive FROM. This allowed the virtual recreation of femur position at measured limiting FROM manoeuvres in hip motion simulation as shown in Fig. 3a and b.

However, the accuracy of the registration of the FROM to hip simulation relied on the estimation of the centre point positions of pelvis and femur reference spheres (i.e., PRSs and FRSs) obtained from both the CT scans and MoveInspect measurements. This was investigated by comparing (a) the diameter of the PRSs and FRSs and (b) the distances between the ith sphere centre to jth sphere centre as follows: dij for pelvis and $Ldij$ or $Rdij$ for left and right femur respectively. In addition, the impact of registration errors on the calculation of decomposed FROM values was investigated by randomly varying each component of the centres (i, j and k) of PRSs and FRSs within the ranges of [−0.5, 0.5] mm, [−1, 1] mm, and [−2, 2], and recalculate the decomposed FROM values.

2.5. Determination of corresponding BROM

After registering the measured limiting passive FROM (Fig. 3a) in the CT-based hip joint simulation (as explained in Section 2.4), the three-dimensional (3D) position and orientation of the femur relative to the pelvis were recreated computationally for each FROM position (Fig. 3b). This registration process helped to assess the accuracy of BROM in representing the actual limiting FROM. The detection of bony impingement was carried out at the specific position corresponding to the passive limiting FROM of the femur. Each limiting FROM was decomposed into three angular motions as described in Section 2.4. Among these, one motion component acted as the variable or leading component. For instance, in the case of maximum flexion FROM, flexion served as the leading motion component, while some abduction/adduction and internal/external rotation were associated with the flexion movement, as the motion was performed manually prior to the registration. If a bony impingement was detected at the limiting FROM position, it was concluded that restriction was resulted from bony impingement. Alternatively, in cases where no impingement was observed, the variable/leading motion component was systematically augmented by 0.5° increments while keeping the other two decomposed angular motions unchanged. This process continued until bony impingement was detected (Fig. 3c). Once impingement occurred, the limiting ROM was defined as corresponding BROM, and the disparity between the limiting FROM and BROM indicated the degree of restriction imposed by the soft tissues and ligaments (Fig. 3c).

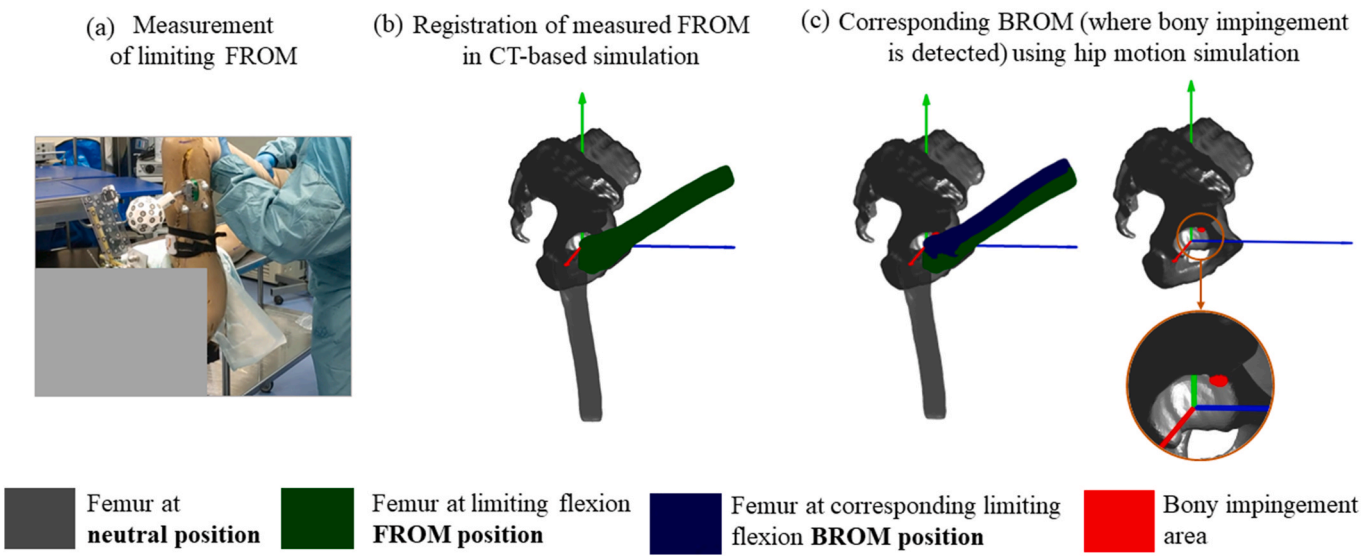

Fig. 3. Representation of the measurement, registration, and simulation workflow of the study. (a) A representative limiting FROM measurement position - limiting flexion, (b) Registration of the experimentally measured limiting FROM position (limiting flexion) in CT-based in-house hip motion simulation (HMS) to reconstruct the position of the femur virtually with respect to pelvis, (c) Calculation of corresponding limiting BROM position of femur (limiting flexion BROM) by identifying the bony impingement using in-house hip motion simulation (HMS).

2.6. Estimation of FHJC and its effect on ROM computation

Initial non-limiting circumducted motion (or conical motion) of the femur (Section 2.2) was used to determine the FHJC. First, the circumducted FROM was registered in CT-based hip motion simulation (Section 2.4) and the centre of rotation (CoR) of the conical motion was calculated using centre transformation technique (CTT) [31–33] which is highly regarded for its reliability and ease of application in orthopaedic navigation systems, particularly when compared to alternative approaches [32,34]. One of the key advantages of CTT is its ability to directly utilise rotational-translational data obtained from a coordinate system defined by markers attached to the femur and pelvis segments in an orthopaedic application [34]. The estimated FHJC was then compared with AHJC to compute their positional difference. In addition, the effect on computed BROM due to the shift in the centre of rotation from the AHJC to FHJC was investigated for four hip motions as follows: (a) maximum flexion, (b) maximum abduction, (c) maximum internal rotation (IR) at 90° flexion (Flex) with neutral abduction/adduction, (d) maximum external rotation (ER) at 20° extension (Extn) with neutral abduction/adduction.

3. Results

3.1. Measured passive FROM and corresponding BROM

Table 1 presents a comparison of limiting FROM and corresponding BROM values in this study with those found in the literature. It is important to note that the literature values were obtained from the studies that exclusively focused on either FROM measurements only or BROM simulation alone. Consequently, the novelty of the current study was its detailed exploration of evaluating BROM by comparing it with measured FROM (last column of Table 1), which had not been extensively examined in the existing literature. In Table 1, columns 2 and 4 display the mean and standard deviation of the measured FROM and the corresponding computed BROM for the four hips. The last column provides the mean and standard deviation of the differences between these values. Additionally, a comparison between the measured FROM and literature values is presented in columns 2 and 3 of Table 1. Similarly, the comparison between BROM values and literature is shown in columns 4 and 5.

Figs. 4 and 5 illustrate the difference between the measured limiting FROM and corresponding computed BROM for each hip case. Fig. 4a1, b1 and c1 show the measured limiting FROM and corresponding BROM for maximum flexion, maximum extension, and maximum abduction respectively. Each motion was performed for each hip case with three repeated runs. Fig. 4a2, b2 and c2, therefore, explicitly depict the difference between BROM and FROM for each case, averaged over the three repeated runs. The other two decomposed angular motions that were associated with the leading motion (for example, abd/add and IR/ER were two angular motions that were associated with leading motion component maximum flexion) are detailed in Appendix A. It was observed that the difference between functional and computed flexion was below 12° for all cases (Fig. 4a1 and a2). The average difference in flexion between FROM and BROM for all cases was 3.0° ± 4.1° (Table 1). The difference between FROM and BROM for extension was more than 40° for all runs and cases (Fig. 4b1 and b2), with a mean difference and variation of 53.2° ± 9.5° (Table 1). The difference in abduction was between 10° and 20° for all cases except case 3 where the differences were less than 10° (Fig. 4c1 and c2). Including all the cases and runs, the differences in abduction was observed to be 13.5° ± 4.6° (Table 1).

The measured functional IR and the computed IR during deep flexion, with varying levels of abduction and adduction, were consistently below 10° (Fig. 5a1 to c2). Specifically, the average differences and deviations for minimal abduction/adduction, maximal abduction, and maximal adduction, when considering all runs and cases, were found to be 3.0° ± 2.9°, 5.7° ± 3.6°, and 6.2° ± 2.9° (Table 1), respectively. Differences between the measured functional ER and the computed ER during extension were always below 15° with average differences 9.0° ± 4.1° (Table 1 and Fig. 5d1 and d2).

It was observed that the FROM and BROM values are same for the maximum flexion values in Case 3 (2 runs) and Case 4 (all 3 runs) (Fig. 4a2), as well as the maximum IR at deep flexion for Case 3 (1 run) and Case 4 (all 3 runs) (Fig. 5a2). It indicates that the bony impingement may occur between the femur and pelvis during specific hip motions in certain cases of healthy and normal hips.

3.2. Variation in reference spheres measurement and measured FROM

Fig. 6 illustrates the variation in diameter measurements of pelvis

Table 1
Compare limiting FROM and corresponding BROM values in this study with literature values.

Manoeuvres Name	FROM this study (°)	FROM Literature (°)	BROM this study (°)	BROM Literature (°)	Difference between BROM and FROM (Novelty in this study) (°)
1. Max Flexion	108.1 ± 5.1	110 ± 15 [35] 112.1 ± 11.3 [36] 103.6 ± 9.0 [37]	111.1 ± 8.1	121 ± 11.8 [24] 122 ± 11 [38] 122.5 ± 11.1 [39]	3.0 ± 4.1
2. Max Extension	20.8 ± 11.9	16.5 ± 6 [35] 19.7 ± 6.1 [22]	74.1 ± 20.2	58 ± 20.4 [24] 61 ± 32 [38] 57.1 ± 19.9 [39]	53.2 ± 9.5
3. Max Abduction	37.7 ± 3.9	38.7 ± 8 [35] 39.3 ± 7.4 [36] 36.9 ± 8.32 [37]	51.2 ± 6.7	63 ± 11.1 [24] 61 ± 14 [38]	13.5 ± 4.6
4. Max IR at deep flexion with minimal abduction/adduction	13.5 ± 5.4	28.2 ± 11 [35] 24.3 ± 9.1 [22] 18.6 ± 9.4 [37]	16.5 ± 7.7	35 ± 12 [24] 36 ± 16 [38] 43.1 ± 15.2 [39]	3.0 ± 2.9
5. Max IR at deep flexion with maximal abduction	21.9 ± 3.6	–	27.7 ± 3.9	–	5.7 ± 3.6
6. Max IR at deep flexion with maximal adduction	11.9 ± 3.1	–	18.1 ± 5.2	–	6.2 ± 2.9
7. Max ER at extension	31.7 ± 9.3	38.5 ± 8.7 [40]	40.7 ± 9.4	41 ± 22 [38] 42.3 ± 15.1 [39]	9.0 ± 4.1

Mean ± standard deviation.

and femur reference spheres (PRSs and FRSs) obtained from post-experiment CT scans and MoveInspect measurements. All the Alufix 'reference balls', representing PRSs and FRSs, have a nominal diameter of 18 mm. Interestingly, the average diameter estimation from the CT scans consistently exceeded that of the MoveInspect measurements. The discrepancy between the calculated diameters of PRSs and FRSs, derived from the CT scans and MoveInspect measurements, was found to be 0.5 ± 0.2 mm. However, the accuracy of the registration of the FROM to hip simulation relied on the estimation of the centre point positions of PRSs and FRSs obtained from both the CT scans and MoveInspect measurements. Notably, the differences in lengths between the centres of PRSs and FRSs were minimal, measuring only 0.1 ± 0.1 mm. These differences were considerably lower compared to the disparities observed in diameter calculations.

Following the registration process, the positional differences of the PRS centres obtained from CT and MoveInspect-based calculations for 4 hip cases were as follows: (a) PRS1: 0.0 ± 0.0 mm, (b) PRS2: 0.06 ± 0.03 mm, (c) PRS3: 0.27 ± 0.16 mm. Similarly, the difference for FRS centres were: (a) FRS1: 0.0 ± 0.0 mm, (b) FRS2: 0.18 ± 0.09 mm, (c) FRS3: 0.31 ± 0.14 mm. On the other hand, the impact of registration errors on the calculation of decomposed FROM values were found to be on average 0.7°, 1.7°, and 4.4° due to the random change in position of each component of the centres (i, j and k) of pelvis and femur reference spheres (PRSs and FRSs) within the ranges of [−0.5, 0.5] mm, [−1, 1] mm, and [−2, 2] mm respectively.

3.3. Comparison of FHJC and AHJC and their impact on computed BROM

In Fig. 7a, the green femurs depict the positions of femur during non-limiting passive circumducted motion recorded in a measurement run, achieved after the registration of measurement data in CT-based HMS. The tri-coloured frames represent the coordinate systems associated with femoral adaptors, referred FACSs, which were measured using the AICON MoveInspect XR8 system. The positions of the FHJC, as determined from 'non-limiting' passive circumducted motions and AHJC, calculated based on the best fit sphere centre of the femoral head, is represented in Fig. 7b. The distance between the FHJC and the AHJC for the four cases is represented in Fig. 7c with an average distance of 3.1 ± 1.2 mm calculated across these cases. In Case 1, the error between the FHJC and AHJC was greater compared to the other three cases.

Fig. 8 illustrates the differences in BROM estimation due to the use FHJC as centre of rotation in HMS instead of AHJC for the four cases. It was observed that the differences were more pronounced in case 1 compared to the other cases. Furthermore, the impact on abduction was minimal in comparison to the other three hip motions. In summary, the differences, considering all four cases, were as follows: (a) Flexion: 7.7° ± 5.6°, (b) abduction: 3.2° ± 1.9°, (c) Max IR at 90° Flex: 6.1° ± 2.9°, and (d) 5.5° ± 2.3°.

4. Discussion

This study aimed to evaluate a CT-based hip motion simulation (HMS) for calculating BROM and assess its sensitivity to the choice of the functional or anatomical hip joint centre (FHJC and AHJC) as the rotation centre of hip motion. This evaluation was conducted by registering cadaver-based passive FROM measurement data into the HMS. The novel aspects of the study were as follows. Firstly, a precise measurement procedure was developed to capture cadaver-based passive limiting and non-limiting FROM of hip with the capability to register the measured data into a CT-based HMS. Secondly, the registration capability facilitates a direct comparison between the measured FROM and the corresponding BROM, allowing for the assessment of its reliability. It was observed that there were minimal differences between FROM and BROM in maximum flexion (3.0° ± 4.1°) and IR at deep flexion with any amount of abduction or adduction (3.0° ± 2.9°, 5.7° ± 3.6°, and 6.2° ± 2.9° respectively). However, greater differences were found in extension (53.2° ± 9.5°) indicating larger constraints imposed by soft-tissue and ligaments. Moderately differences were found in abduction (13.5° ± 4.6°), and ER during extension (9.0° ± 4.1). Thirdly, the study revealed that bony impingement occurred in the hips of individuals with normal and healthy anatomy during specific motions, such as flexion and deep flexion internal rotation. Fourthly, the study included an analysis of the registration process consistency to examine its impact on the calculated BROM. Finally, the positional difference between FHJC and AHJC was explored, with a measured disparity of 3.1 ± 1.2 mm, and for the first time, their impact on the calculated BROM for four manoeuvres was examined and it was found to be in the range of 1°–13°. This finding emphasised that AHJC can effectively serve as a reliable approximation of FHJC. Each of these research findings are discussed in the subsequent sections, aiming to underscore their theoretical and practical implications and to compare them with previous research findings along with study limitation and future research scope.

It was found that the measured passive limiting FROM was comparable with measurement values reported in the literature except max IR values at deep flexion with neutral abduction/adduction (Table 1)

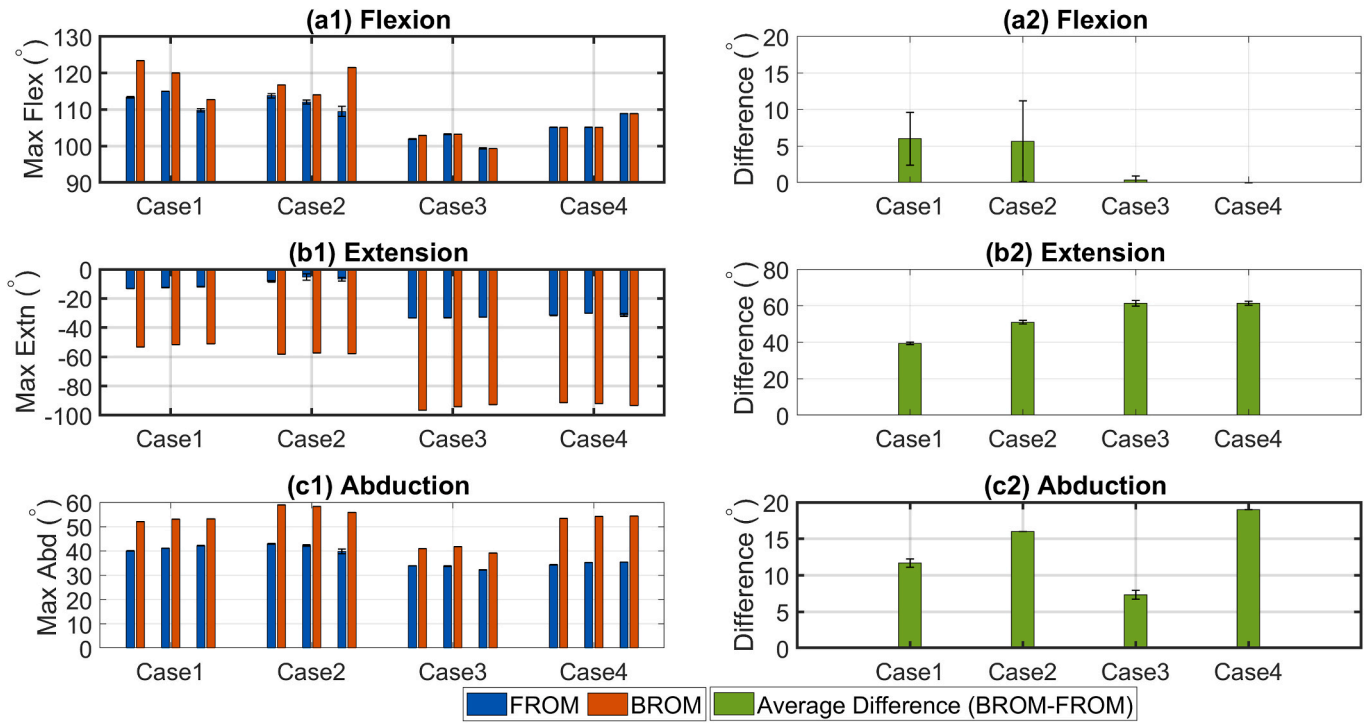

Fig. 4. Comparison of passive limiting FROM and corresponding computed BROM. (a1, b1, c1) depict both FROM and corresponding BROM for maximum flexion, maximum extension, and maximum abduction respectively for each case/specimen, and each case includes three repeated runs. (a2, b2, c2) represent the average difference between BROM and FROM for flexion, extension, and abduction respectively for each case/specimen.

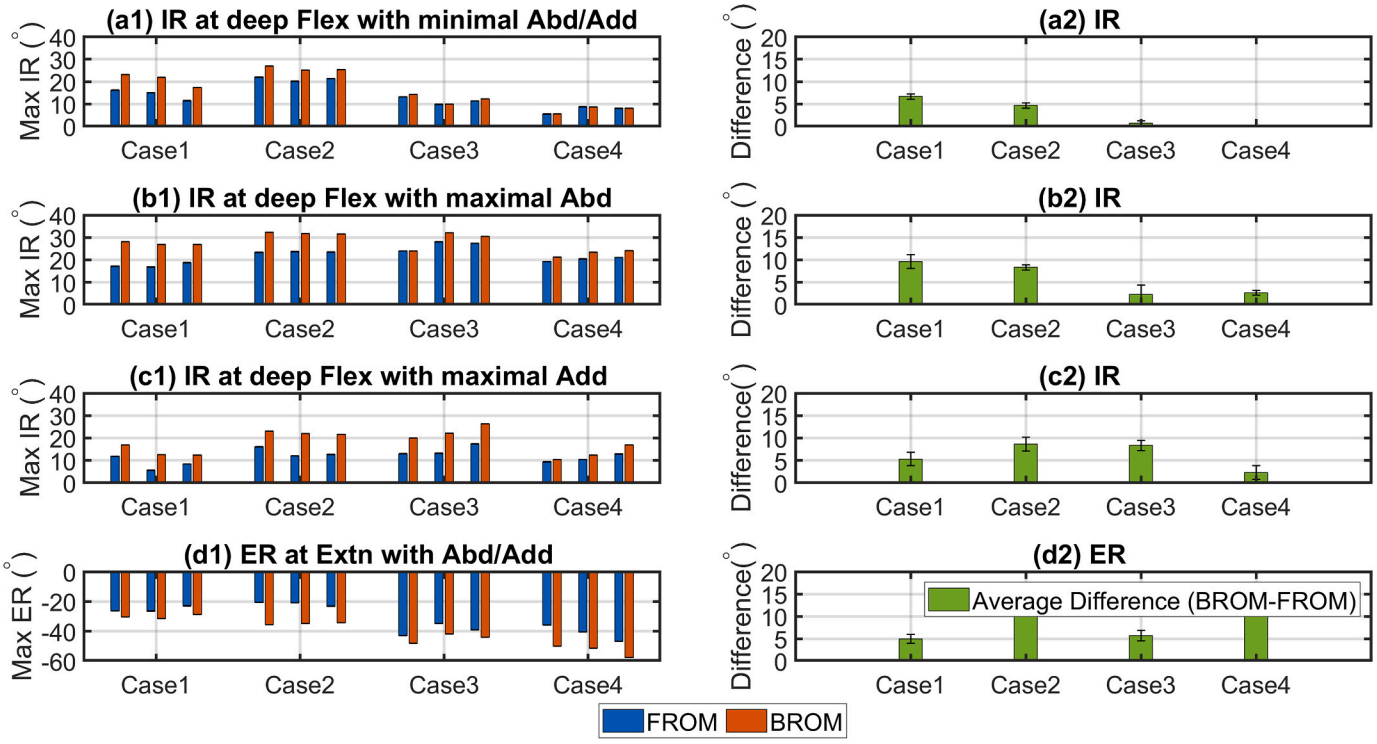

Fig. 5. Comparison of passive limiting FROM and corresponding computed BROM. (a1, b1, c1, d1) depict both FROM and corresponding BROM for following motions: maximum IR at deep flexion with minimal Abd/Add, maximum IR at deep flexion with maximal abduction, maximum IR at deep flexion with maximal adduction, and maximum ER at extension with Abd/Add for all 4 cases/specimen and each case includes 3 repeated runs. (a2, b2, c2, d2) represent the average difference between BROM and FROM for each case due to repeated runs.

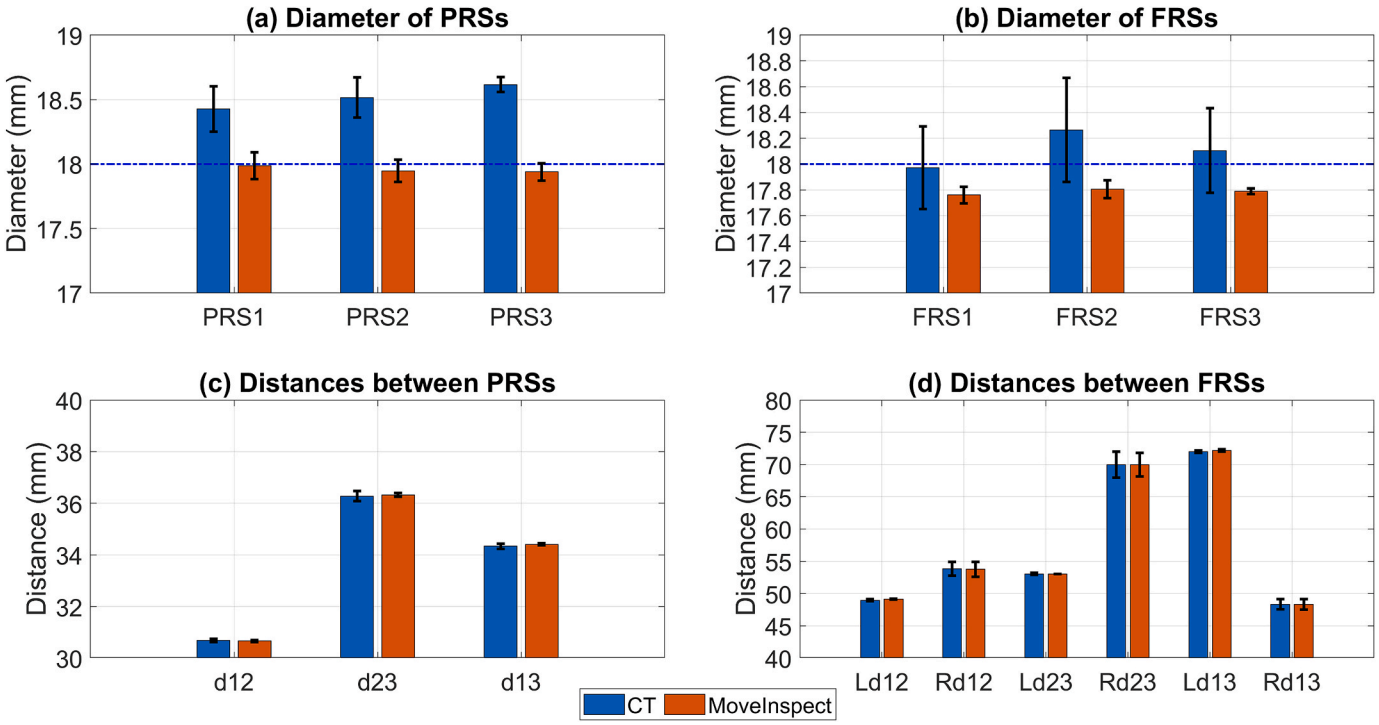

Fig. 6. Differences in reference sphere measurements from CT-scan and AICON MoveInspect XR8. (a) Differences in the RRSs diameter where blue line depicts nominal diameter of the PRSs, (b) differences in FRSs diameters where blue line depicts nominal diameter of the FRSs, (c) differences in distances between sphere centres of PRSs where dij represented the distance between ith centre to jth centre (i, j = 1, 2, 3) and (d) differences in distances between sphere centres of FRSs where dij represented the distance between ith centre to jth centre (i, j = 1, 2, 3) and L and R represented left or right femur respectively.

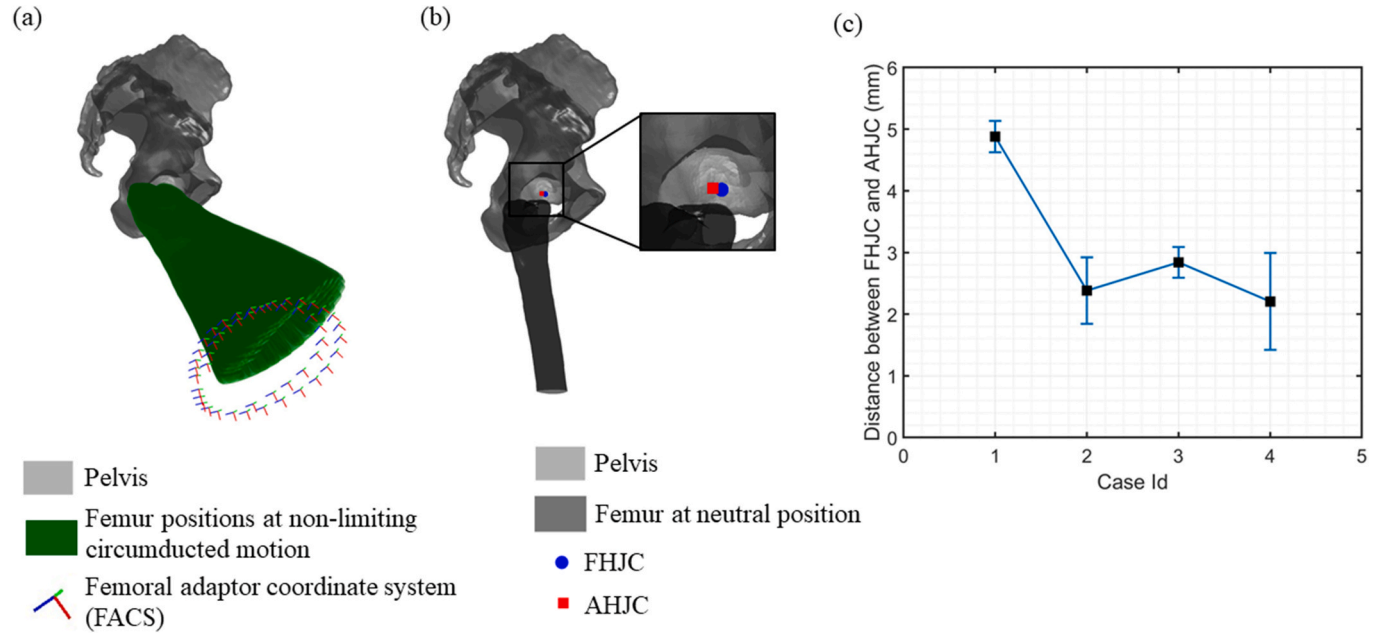

Fig. 7. (a) Representation of non-limiting circumducted passive FROMs after registering the measurement data with the CT-based hip motion simulation. The green femurs represent all non-limiting circumducted motions performed during a measurement run. The tri-colour frames represent the actual femoral adaptor coordinate systems (FACSs) that were tracked using AICON MoveInspect XR8. (b) Difference in position of the FHJC, estimated from the non-limiting circumducted passive FROMs and AHJC. (c) The distances between FHJC and AHJC for 4 cases.

where relatively lower values were observed. This was due to experimental results from hip case 3 and 4 where additional amount of (3°–10°) adduction (Figure A.2 in Appendix A) was involved while performing max IR manoeuvres at deep flexion with neutral abduction/adduction. This additional amount of adduction may lead to reduction in limiting IR values as evident from the work of Kubiak-Langer, Tannast [41]. It was observed that the calculated BROM were consistent with the previous simulation studies of normal hips [21,24,25,38,39] (Table 1). For instance, the simulated BROM values for flexion, extension, and abduction were found to be 111.1° ± 8.1°, 74.1° ± 20.2°, and 51.2° ±

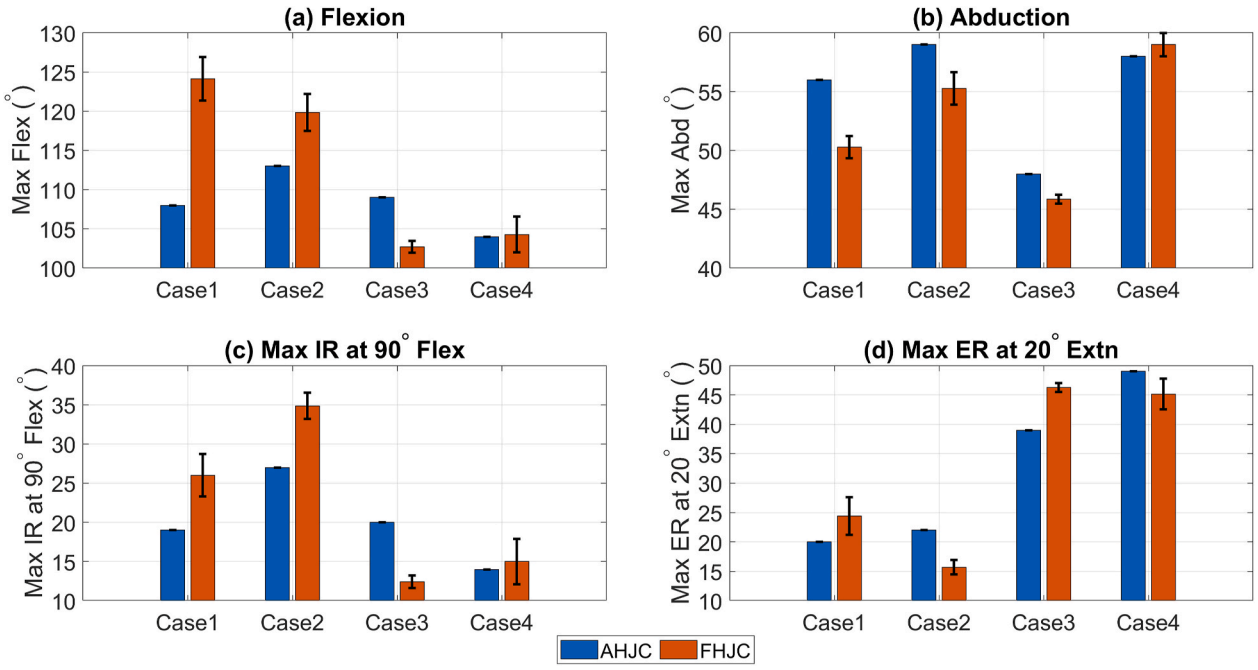

Fig. 8. Change in limiting BROM calculation due to the use of FHJC and AHJC as HJC in hip simulation. (a) Maximum flexion, (b) maximum abduction, (c) maximum internal rotation (IR) at 90° flexion (Flex) with neutral Abduction/Adduction, (d) maximum external rotation (ER) at 20° extension (Extn) with neutral abduction/adduction.

6.7°, respectively. These values align closely with previously reported findings of flexion (122.5° ± 11.1°) [32,33], extension (58.0° ± 20.4°) [42] or (61.3° ± 32.0°) [38], and abduction (61.0° ± 14.0°) [38,42]. However, one notable difference in this study was that the computed BROM values for manoeuvres 1 to 7 (Table 1) were not purely isolated joint motions (Section 2.5). Due to the objective of calculating the corresponding BROM to a limiting FROM, there were minor contributions of other motions to the determination of the leading BROM values (Section 2.5). For example, the flexion value was always associated with some amount of abduction/adduction and IR/ER in this study (Appendix A). This was primarily due to the manual execution of the FROM. On the other hand, manual passive motion by experienced hip surgeons was essential to realistically identify the limiting motion by adjusting the applied manual forces. This was the advantages of using manual execution instead of utilising a robot or a force-based limiting motion detection system as the value of the limiting force was unknown. This was in contrast to a simulation-only studies where pure flexion values can be easily calculated by keeping abduction/adduction and IR/ER to 0°. As a result, the BROM values reported in the study (such as max Flexion) (manoeuvres 1 to 7 in Table 1) were not exactly same to the BROM values included in Table 1 from literature. However, the study's findings indicated consistency with previous research regarding the FROM and BROM of normal hips, although some additional motion components were observed due to the nature of the experimental setup and the objective of the study. It is important to note that the literature values were obtained from the studies that exclusively focused on either FROM measurements only or BROM simulation alone. Consequently, the novelty of the current study was its detailed examination in evaluating BROM by comparing it with measured FROM (last column of Table 1), which had not been extensively examined in the existing literature.

The observed differences between limiting FROM and the corresponding BROM for the seven hip motions examined in this study align with clinical observations (Table 1, Figs. 4 and 5). Specifically, the differences in deep flexion and internal rotation during deep flexion across various levels of abduction and adduction fell within the range of 0°–20°. This suggests that the impact of soft tissues and ligament constraints is relatively small in these cases. However, the differences between the simulated and functional extension values ranged from 53.2° ± 9.5°, indicating a considerable restriction caused by soft tissues, ligaments, and fat. One important finding of the study was that the bony impingement can occur between the femur and pelvis during some hip motions of a healthy, normal hip. This was evident from the maximum FROM flexion values of Case 3 (2 runs) and 4 (all runs) (Fig. 4a2) as well as maximum IR at deep flexion for case 3 (1 run) and case 4 (all runs) (Fig. 5a2). The obtained results were consistent with a previous study [22]. Therefore, the Flexion Adduction Internal Rotation (FADIR) diagnostic test, where hip is fully flexed or 90° flexion along with adduction and IRs to assess the existence of Femoroacetabular impingement (FAI) could lead to false positive diagnosis for some patients with normal hip anatomy.

Following the registration process, the measured FROM was decomposed into three Euler's angles to calculate the flex/extn, abd/add and IR/ER associated with the FROM. Therefore, the accuracy of the decomposed FROM values relied on the precision of the registration process, which, in turn, depended on the segmentation and identification of the centres of the PRSs and FRSs. It was observed that the change in position of each component of the centres (i, j, and k) within the specified ranges of [−0.5, 0.5] mm, [−1, 1] mm, and [−2, 2] mm, the corresponding average changes in the decomposed FROM were 0.7°, 1.7°, and 4.4° respectively. This highlighted the accuracy and repeatability of the developed registration process. A few previous studies measured selected manoeuvres in cadavers and registered them in simulation to calculate decomposed hip motions [21,23,25]. However, none of these studies investigated the sensitivity of the results due to the variation in the registration process. This is the first time the effect was investigated.

The difference between FHJC and AHJC centre combining all cases was found to be 3.1 ± 1.2 mm where Case 1 showed the largest difference. The observed results on fFHJC were found to be in accordance with a previous publication [34]. The difference in location of AHJC and FHJC resulted in differences in limiting BROM estimation. It was observed that the difference could be more than 10° in some hip motions when FHJC is used as rotation centre in the simulation instead of AHJC. Hence, it demonstrated that AHJC could serve as a valid approximation

of FHJC. However, it is noteworthy that the difference between FHJC and AHJC in this study was an order of magnitude lower compared to other in-vivo studies where trackers were attached to the skin surface (resulting in artifact errors ranging from 18 to 32 mm) [43]. Consequently, a higher error in evaluating the FHJC can significantly affect the determination of the limiting BROM when compared to the values calculated using the AHJC.

The study had several limitations that need to be acknowledged. Firstly, the passive FROM was manually performed, making it impossible to precisely replicate each motion during different runs due to the lack of an in-process monitoring system. Consequently, direct comparisons between motions were challenging as there were variations in the degrees of other motions involved, even within different runs of the same motion. However, it provided additional variations in nearby limiting motions. Secondly, the identification of the limiting passive FROM was based on the assessment of an experienced surgeon instead of utilising a robot or a force-based impingement detection system. The authors made this decision because the surgeon's 25 years of experience was considered more reliable in accurately identifying the limiting motion compared to using a robot, where the value of the limiting force was unknown. Additionally, using a robot could potentially lead to overestimation of the limiting force, which might cause subluxation. Finally, the study did not incorporate the translation of the femoral head within the acetabulum during virtual hip motion in the simulation as translation of HJC during FROM measurement was not captured. Therefore, degree of hip motion restriction was determined by assuming a constant femoral head centre in the collision detection process. Nevertheless, it is expected that the research findings would remain consistent. The methodology proposed in this study and its findings hold significant potential for future research aimed at further exploring the relationship between BROM and FROM through additional experiments covering a wide range of hip motions, as well as gaining a greater understanding of soft tissue and ligament impingement and constraints during hip motions. This would ultimately facilitate the identification of FROMs that can be reliably predicted from computed BROMs through CT-based HMS. As a result, these BROMs would serve as a close representation of the actual FROMs, which are difficult to measure in clinical setting for each patient. This approach would subsequently enhance surgical planning due to the use of personalised BROMs data as target values for hip replacement procedures. It would, therefore, eliminate the dependence on population-based 'normal' target ROM values generally used in state-of-the-art hip surgical pre-planning simulation. These values can be inadequate for patients whose hip motion characteristics never conformed to so-called 'normal' range.

5. Conclusion

In this study, the assessment of CT-based BROM simulation was performed by registering passive limiting FROM measurement data into a CT-based hip simulation. The differences between calculated BROM and measured FROM was minimal in maximum flexion ($3.0^\circ \pm 4.1^\circ$) and maximum IR at deep flexion with varying level of abduction and adduction ($3.0^\circ \pm 2.9^\circ$, $5.7^\circ \pm 3.6^\circ$, and $6.2^\circ \pm 2.9^\circ$), whereas higher differences were observed in extension movement ($53.2^\circ \pm 9.5^\circ$). It was observed that the bony impingement can occur in healthy normal hips as evident from the observed maximum flexion and maximum IR at deep flexion movements for two cases. Furthermore, the study determined that the average difference in location between the FHJC and AHJC was 3.1 ± 1.2 mm. Consequently, this led to differences in the calculation of the limiting BROM, ranging from 1° to 13°. Therefore, it was concluded that the AHJC could serve as a valid approximation of FHJC. However, artifact or error in the measurement process of the FHJC can result in higher differences in the estimated BROM in comparison to those calculated using AHJC. Therefore, all these findings from this study contribute to a greater understanding of the applicability and reliability of computed BROM as a valuable tool in clinical decision-making processes, such as pre-operative planning of hip replacement surgery.

Declaration of competing interest

The authors declare that they have no known competing financial interests or personal relationships that could have appeared to influence the work reported in this paper.

Acknowledgement

The study received funding from Corin Group, UK. We would like to extend our appreciation to Hexagon UK and AICON, Germany for their valuable support in enabling us to utilise the AICON MoveInspect XR8 system effectively. Additionally, we express our sincere gratitude to Dr. Simon Ford and his team at the West Midlands Surgical Training Centre at University Hospital Coventry and Warwickshire NHS Trust for their kind assistance in preparing the cadaver specimens and providing continuous support throughout the experimental procedures. Furthermore, we would like to acknowledge the contributions of Mr. Joseph Benjamin and Mr. Mike Donnelly from our team for their invaluable support in arranging the experiment kits and fixtures.

Appendix A

Figs. A.1 and A.2 illustrate the difference between the measured limiting FROM and corresponding computed BROM. The plot that is shaded with a grey background depict the disparity between the leading/variable motion component of FROM and BROM, while the other two plots in the same row demonstrates the other two decomposed angular motions. The plot with grey background is actually included in the main manuscript (Figs. 3 and 4). For example, a3, b3 and c3 plots show three decomposed angular motions that were associated with maximum abduction, namely neutral flex/extn, maximum abduction (leading motion) and neutral IE/ER, respectively.

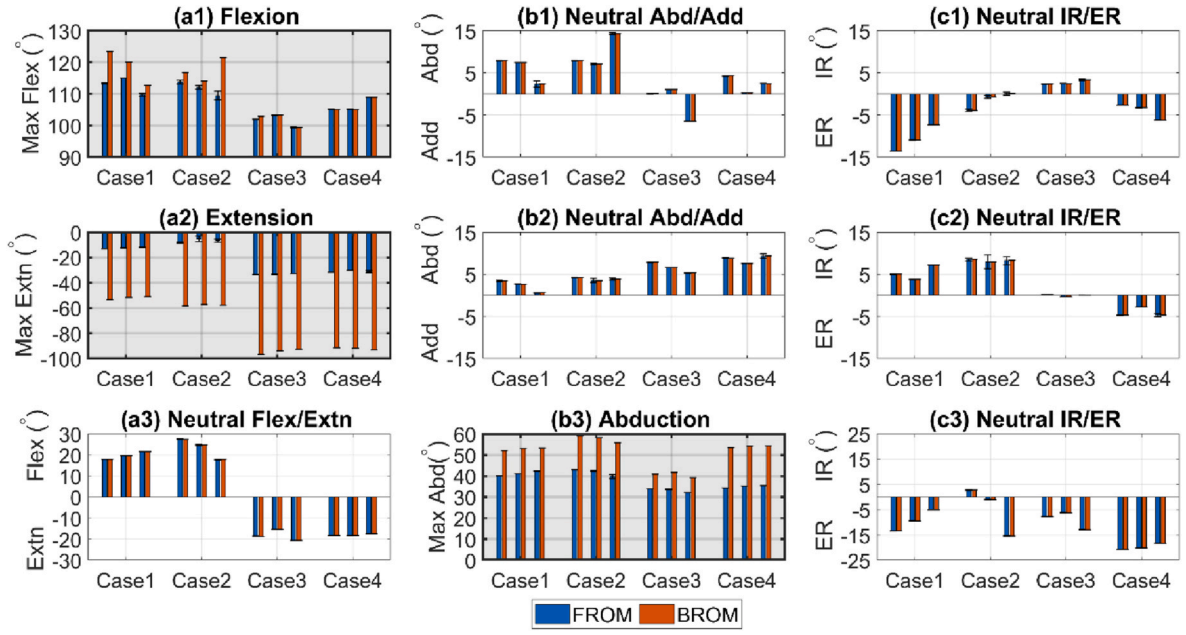

Fig. A.1. Comparison of passive limiting FROM and corresponding computed BROM. The plots that are shaded with a grey background depict the disparity between the FROM and BROM, while the other two plots in the same row illustrate the other two decomposed angular motion. (a1, b1, c1) depict the max flexion, neutral abd/add and neutral IR/ER respectively associated max flexion motion; (a2, b2, c2) represent the max extension, neutral abd/add and neutral IR/ER respectively associated max extension motion; (a3, b3, c3) illustrate the neutral flex/extn, maximum abduction and neutral IR/ER respectively associated max abduction motion.

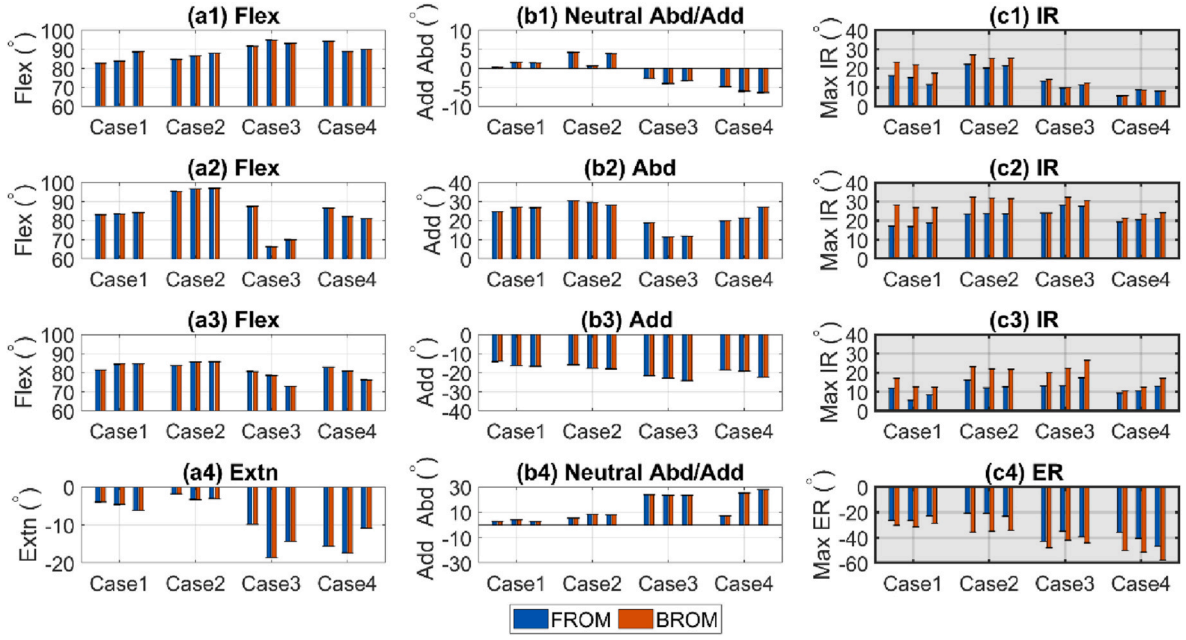

Fig. A.2. Comparison of passive limiting FROM and corresponding computed BROM. The plots that are shaded with a grey background depict the disparity between the FROM and BROM, while the other two plots in the same row illustrate the other two decomposed angular motion. (a1, b1, c1) depict deep flexion, neutral abd/add and maximum IR respectively associated max IR at deep flexion motion; (a2, b2, c2) represent deep flexion, higher abduction and maximum IR respectively associated max IR at deep flexion with higher abduction motion; (a3, b3, c3) represent deep flexion, higher adduction and maximum IR respectively associated max IR at deep flexion with higher adduction motion; (a4, b4, c4) represent extension, neutral abduction/adduction and maximum ER respectively associated max ER at extension.

References

[1] M.H. Huo, J. Parvizi, B.S. Bal, M.A. Mont, What's new in total hip arthroplasty, J. Bone Joint Surg. Am. 91 (10) (2009) 2522–2534.
[2] D. Bennett, et al., Temporospatial parameters of hip replacement patients ten years post-operatively, Int. Orthop. 33 (5) (2009) 1203–1207.
[3] A. Enocson, et al., Dislocation of total hip replacement in patients with fractures of the femoral neck, Acta Orthop. 80 (2) (2009) 184–189.
[4] H. Miki, et al., Detecting cause of dislocation after total hip arthroplasty by patient-specific four-dimensional motion analysis, Clin. Biomech. 28 (2) (2013) 182–186.
[5] C.F. Scifert, et al., Experimental and computational simulation of total hip arthroplasty dislocation, Orthop. Clin. N. Am. 32 (4) (2001) 553–567, vii.
[6] D.D. D'Lima, et al., The effect of the orientation of the acetabular and femoral components on the range of motion of the hip at different head-neck ratios, J. Bone Joint Surg. Am. 82 (3) (2000) 315–321.

[7] M.E. Nadzadi, et al., Kinematics, kinetics, and finite element analysis of commonplace maneuvers at risk for total hip dislocation, J. Biomech. 36 (4) (2003) 577–591.
[8] K.R. S, et al., Outcome of treatment for dislocation after primary total hip replacement, British volume, J. Bone Joint Surg. 91-B (3) (2009) 321–326.
[9] T. Shoji, et al., Factors affecting the potential for posterior bony impingement after total hip arthroplasty, Bone Joint Lett. J 99-b (9) (2017) 1140–1146.
[10] P.F. Lachiewicz, E.S. Soileau, Low early and late dislocation rates with 36- and 40-mm heads in patients at high risk for dislocation, Clin. Orthop. Relat. Res. 471 (2) (2013) 439–443.
[11] F.E. Rowan, B. Benjamin, J.R. Pietrak, F.S. Haddad, Prevention of dislocation after total hip arthroplasty, J. Arthroplasty 33 (5) (2018) 1316–1324.
[12] A. Palit, et al., Subject-specific surgical planning for hip replacement: a novel 2D graphical representation of 3D hip motion and prosthetic impingement information, Ann. Biomed. Eng. 47 (7) (2019) 1642–1656.
[13] J. Schmid, et al., MyHip: supporting planning and surgical guidance for a better total hip arthroplasty : a pilot study, Int. J. Comput. Assist. Radiol. Surg. 10 (10) (2015) 1547–1556.
[14] G.A. Turley, M.A. Williams, R.M. Wellings, D.R. Griffin, Evaluation of range of motion restriction within the hip joint, Med. Biol. Eng. Comput. 51 (4) (2013) 467–477.
[15] K.H. Widmer, B. Zurfluh, Compliant positioning of total hip components for optimal range of motion, J. Orthop. Res. 22 (2004).
[16] L. Petrolo, D. Testi, F. Taddei, M. Viceconti, Effect of a virtual reality interface on the learning curve and on the accuracy of a surgical planner for total hip replacement, Comput. Methods Progr. Biomed. 97 (1) (2010) 86–91.
[17] A. Palit, et al., Femur First navigation can reduce impingement severity compared to traditional free hand total hip arthroplasty, Sci. Rep. 7 (1) (2017) 7238.
[18] O. Kessler, et al., Bony impingement affects range of motion after total hip arthroplasty: a subject-specific approach, J. Orthop. Res. 26 (4) (2008) 443–452.
[19] A. Palit, et al., Prediction and visualisation of bony impingement for subject specific total hip arthroplasty*, in: 2019 41st Annual International Conference of the IEEE Engineering in Medicine and Biology Society (EMBC), 2019.
[20] A. Palit, et al., Bone-to-Bone and implant-to-bone impingement: a novel graphical representation for hip replacement planning, Ann. Biomed. Eng. 48 (4) (2020) 1354–1367.
[21] A. Palit, R. King, J. Pierrepont, M.A. Williams, Development of bony range of motion (B-ROM) boundary for total hip replacement planning, Comput. Methods Progr. Biomed. 222 (2022), 106937.
[22] S. Han, et al., The continuum of hip range of motion: from soft-tissue restriction to bony impingement, J. Orthop. Res. 38 (8) (2020) 1779–1786.
[23] G.A. Turley, S.M. Ahmed, M.A. Williams, D.R. Griffin, Establishing a range of motion boundary for total hip arthroplasty, Proc. Inst. Mech. Eng. H 225 (8) (2011) 769–782.
[24] M. Tannast, et al., Noninvasive three-dimensional assessment of femoroacetabular impingement, J. Orthop. Res. 25 (1) (2007) 122–131.
[25] T.-C. Chang, H. Kang, L. Arata, W. Zhao, A pre-operative approach of range of motion simulation and verification for femoroacetabular impingement, Int. J. Med. Robot. Comput. Assist. Surg. 7 (3) (2011) 318–326.
[26] N. Nakamura, et al., Effect of soft-tissue impingement on range of motion during posterior approach Total Hip Arthroplasty: an in vivo measurement study, Comput. Assist. Surg. 21 (1) (2016) 132–136.
[27] M. Woerner, et al., Soft tissue restricts impingement-free mobility in total hip arthroplasty, Int. Orthop. 41 (2) (2017) 277–282.
[28] M.A. Röling, et al., A quantitative non-invasive assessment of femoroacetabular impingement with CT-based dynamic simulation - cadaveric validation study, BMC Muscoskel. Disord. 16 (1) (2015) 50.
[29] G.A. Turley, Graphical representation of range of motion in the assessment of total hip arthroplasty: innovation report, in: WMG, University of Warwick, 2012.
[30] G. Wu, et al., ISB recommendation on definitions of joint coordinate system of various joints for the reporting of human joint motion–part I: ankle, hip, and spine. International Society of Biomechanics, J. Biomech. 35 (4) (2002) 543–548.
[31] S.J. Piazza, A. Erdemir, N. Okita, P.R. Cavanagh, Assessment of the functional method of hip joint center location subject to reduced range of hip motion, J. Biomech. 37 (3) (2004) 349–356.
[32] R.M. Ehrig, W.R. Taylor, G.N. Duda, M.O. Heller, A survey of formal methods for determining the centre of rotation of ball joints, J. Biomech. 39 (15) (2006) 2798–2809.
[33] R.A. Siston, S.L. Delp, Evaluation of a new algorithm to determine the hip joint center, J. Biomech. 39 (1) (2006) 125–130.
[34] N. Lopomo, et al., Evaluation of formal methods in hip joint center assessment: an in vitro analysis, Clin. BioMech. 25 (3) (2010) 206–212.
[35] H. Prather, et al., Reliability and agreement of hip range of motion and provocative physical examination tests in asymptomatic volunteers, PM R 2 (10) (2010) 888–895.
[36] S. Nussbaumer, et al., Validity and test-retest reliability of manual goniometers for measuring passive hip range of motion in femoroacetabular impingement patients, BMC Muscoskel. Disord. 11 (2010) 194.
[37] C.J. Chevillotte, M.H. Ali, R.T. Trousdale, M.W. Pagnano, Variability in hip range of motion on clinical examination, J. Arthroplasty 24 (5) (2009) 693–697.
[38] T.D. Lerch, et al., Patient-specific 3-D magnetic resonance imaging-based dynamic simulation of hip impingement and range of motion can replace 3-D computed tomography-based simulation for patients with femoroacetabular impingement: implications for planning open hip preservation surgery and hip arthroscopy, Am. J. Sports Med. 47 (12) (2019) 2966–2977.
[39] I. Nakahara, et al., Gender differences in 3D morphology and bony impingement of human hips, J. Orthop. Res. 29 (3) (2011) 333–339.
[40] P. Kouyoumdjian, R. Coulomb, T. Sanchez, G. Asencio, Clinical evaluation of hip joint rotation range of motion in adults, J. Orthop. Traumatol.: Surg. Res. 98 (1) (2012) 17–23.
[41] M. Kubiak-Langer, et al., Range of motion in anterior femoroacetabular impingement, Clin. Orthop. Relat. Res. 458 (2007) 117–124.
[42] T.D. Lerch, et al., Femoroacetabular impingement patients with decreased femoral version have different impingement locations and intra- and extraarticular anterior subspine FAI on 3D-CT-based impingement simulation: implications for hip arthroscopy, Am. J. Sports Med. 47 (13) (2019) 3120–3132.
[43] H. Kainz, et al., Estimation of the hip joint centre in human motion analysis: a systematic review, Clin. Biomech. 30 (4) (2015) 319–329.
[44] P. Franciosa, D. Ceglarek, VRM simulation toolkit (2016). http://www2.warwick.ac.uk/fac/sci/wmg/research/manufacturing/downloads/.